Initialization-Free Implicit-Focusing (IF²) for Wideband Direction-of-Arrival Estimation

Jake Millhiser, Pulak Sarangi, Piya Pal Department of Electrical and Computer Engineering, University of California, San Diego

Abstract—This paper proposes a novel method to focus or align array manifolds at different frequencies to a single reference frequency in wideband direction of arrival (DOA) estimation. Unlike existing methods, our focusing can be performed without explicitly constructing focusing matrices, or requiring any preliminary DOA estimates. Instead the focusing is done implicitly by obtaining focused measurements as the solution to a rank minimization procedure. This paper also provides theoretical guarantees for exact focusing via rank minimization. We call this procedure Initialization-Free Implicit-Focusing (IF²). Numerical simulations are provided to demonstrate the resilience of IF² in various SNR regimes compared to past and recent wideband DOA recovery methods, and its lack of error saturation in high SNR regimes¹.

Index Terms—Wideband, direction-of-arrival (DOA) Estimation, Focusing, rank minimization

I. INTRODUCTION

The problem of direction-of-arrival (DOA) estimation has long been an important topic with decades of active research due to its extensive range of applications in radar, sonar, array processing, radio astronomy, communications [1–3], among others. Narrowband DOA estimation has been the subject of study for a long time, with many popular methods like MUSIC and ESPRIT seeing wide use [4, 5]. However, in many cases the narrowband assumption is often not valid due to the signal bandwidth being comparable to the carrier frequency [6], and thus wideband DOA estimation becomes unavoidable. A simple way to extend narrowband methods to wideband is to follow incoherent signal subspace techniques (ICSS) [7], in which the wideband signal is split into multiple narrowband signals, allowing narrowband DOA estimation algorithms to be applied individually, and the results averaged. While providing a simple solution in high SNR, ICSS methods are extremely sensitive in low SNR, and easily ruined by a single outlier [8].

In their seminal work, Wang & Kaveh [9] proposed an alternative wideband DOA method called coherent signal subspace (CSS) methods. They demonstrate the existence of (non-unique) focusing matrices which allow for array manifolds at different frequencies to be aligned (or focused) to a single frequency. This allows the use of well-studied narrowband approaches for DOA recovery in a wise manner that exploits the shared DOA's of each of the narrowband signals, while exhibiting better performance at lower SNR's due to coherent

¹This work was supported in part by the Office of Naval Research under Grant ONR N00014-19-1-2256 and ONR N00014-19-1-2227 and in part by the National Science Foundation under Grant NSF CAREER ECCS 1700506, and NSF 2124929.

combining. However, focusing relies on the availability of preliminary coarse DOA estimates. Additionally, poor choice of focusing matrices can yield loss of SNR due to noise amplification or possible alignment of the noise subspace with the coherent signal subspace [10]. To remedy this, it is common to find focusing matrices from the class of unitary matrices, in a method known as rotational signal subspace (RSS) focusing [10]. While this does address problems with SNR loss, it can cause saturation of error as SNR increases (imperfect even when noiseless).

In recent times, compressed sensing (CS) based methods have been developed for Wideband DOA estimation by formulating it as a group sparsity (GS) recovery problem. Unfortunately, GS methods are known to be computationally expensive, which methods like TS-OG [11] attempt to overcome. Focusing matrices can be still helpful in CS problems as a means to reduce the complexity of the GS problem by bringing all measurements to a single common manifold. Motivated by this, DD-F-OG [12] is proposed as a more computationally efficient wideband CS-based method due to its utilization of focusing. However, DD-F-OG still requires coarse DOA estimates, and is not guaranteed to achieve perfect focusing even in the absence of noise.

Our Contributions: We propose a novel approach to focusing that overcomes the above limitations of using focusing matrices. We bypass the need to construct focusing matrices, and instead perform focusing "implicitly" by casting it as a rank minimization problem. We denote this method as Initialization-Free Implicit-Focusing (IF²). We avoid the need to have any initial DOA estimates, nor do we require the use of any grid of DOA's. We also provide theoretical guarantees for exact focusing using this rank minimization procedure. Our procedure additionally remedies any error saturation that occurs in higher SNR which may result from the use of coarse DOA estimates. Numerical simulations show the benefit of our implicit focusing, by demonstrating resilience in low SNR similar to RSS initialized with the knowledge of true DOAs, and the lack of any error saturation in high SNR. We follow the standard convention that for any vector $\mathbf{x} \in \mathbb{C}^N$ and a set $\Omega = \{i_1, i_2, \cdots, i_p\} \subseteq [N]$, the notation $\mathbf{x}_{\Omega} \in \mathbb{C}^p$ denotes a subvector of **x** given by $[\mathbf{x}_{\Omega}]_j = [\mathbf{x}]_{i_j}, 1 \leq j \leq p$.

II. PROBLEM FORMULATION AND BACKGROUND

Consider the problem of identifying the direction of arrival (DOA) of K wideband signals, $\{s_k(t)\}_{k=1}^K$ with frequency bands supported over $[f_{\text{low}}, f_{\text{high}}]$. Let $\boldsymbol{\theta} = [\theta_1, \theta_2, \cdots, \theta_K]^T$ where θ_k denotes the DOA of the kth source. We consider

an M-sensor uniform linear array (ULA) where the distance between the mth sensor and the reference sensor is given by (m-1)d, $d=\lambda_{\min}/2$ (corresponding to the largest frequency f_{high}). The received signal at the mth sensor at time t can be represented as $x_m(t) = \sum_{k=1}^K s_k(t-\tau_m(\theta_k)) + \tilde{w}_m(t)$ where $\tau_m(\theta_k)$ is a sensor and DOA-dependent time delay (with the first sensor chosen as the reference) obeying $\tau_m(\theta_k) = \frac{md\sin(\theta_k)}{c}$ and $\tilde{w}_m(t)$ is the additive noise. Suppose the measurements $\{x_m(t)\}_{m=1}^M$ are observed over a sufficiently long time window, and sampled at a frequency f_s which is larger than their bandwidths, producing discrete samples $x_m[n], n=0,1,2,\ldots,T$. Most wideband array processing techniques divide the signal $x_m[n]$ into non-overlapping blocks of D samples each, and apply D-point DFT per block [9, 11, 13]. The ith DFT coefficients for the pth block is modeled as:

$$\mathbf{x}_p^{(M)}(f_i) = \mathbf{A}^{(M)}(f_i, \boldsymbol{\theta})\mathbf{s}_p(f_i) + \mathbf{n}_p(f_i)$$
(1)

where $\mathbf{A}^{(M)}(f_i, \boldsymbol{\theta}) := [\mathbf{a}(f_i, \theta_1), \mathbf{a}(f_i, \theta_2), \cdots, \mathbf{a}(f_i, \theta_K)] \in \mathbb{C}^{M \times K}$ is the array manifold at frequency f_i corresponding to ith DFT bin and

$$[\mathbf{a}(f_i, \theta_k)]_m = e^{j\frac{m\pi f_i}{f_{\text{high}}}\sin(\theta_k)}$$
 (2)

Further, $\mathbf{n}_p(f_i)$ denotes the measurement noise, as well as any modeling errors due to finite observation window and/or violation of bandlimited assumptions. For rest of the paper, we will consider only one block (p=1), and suppress the dependence of $\mathbf{x}^{(M)}(f_i)$ on p.

A. Review of Focusing

Historically, the problem of recovering DOA's from wideband signals was addressed by following the coherent signalsubspace method (CSM) [9]. In this procedure, the signal subspaces of each narrowband frequency bin, $i = 1, \dots, D$, are aligned to a single reference frequency, f_{ref} . It was demonstrated in [9] that there are infinite such choices of focusing matrix $\mathbf{T}(f_i)$ which are capable of exact focusing, i.e.

$$\mathbf{A}^{(M)}(f_{\text{ref}}, \boldsymbol{\theta}) = \mathbf{T}(f_i)\mathbf{A}^{(M)}(f_i, \boldsymbol{\theta})$$
(3)

Once these focusing matrices are found, the measurement $\mathbf{x}(f_i)$ could be focused to the reference frequency by applying

$$\mathbf{x}_{\text{focus}}^{(M)}(f_i, f_{\text{ref}}) = \mathbf{T}(f_i)\mathbf{x}^{(M)}(f_i)$$

$$= \mathbf{A}^{(M)}(f_{\text{ref}}, \boldsymbol{\theta})\mathbf{s}(f_i) + \mathbf{T}(f_i)\mathbf{n}(f_i)$$
(4)

In [10], the Rotational Signal Subspace (RSS) focusing matrix was described as a solution to the constrained optimization problem, where $\hat{\theta}$ is an initial DOA estimate:

$$\min_{\mathbf{T}(f_i)} \|\mathbf{A}^{(M)}(f_{\text{ref}}, \hat{\boldsymbol{\theta}}) - \mathbf{T}(f_i)\mathbf{A}^{(M)}(f_i, \hat{\boldsymbol{\theta}})\|_F \qquad (5)$$
s.t.
$$\mathbf{T}^H(f_i)\mathbf{T}(f_i) = \mathbf{I}$$

A solution to (5) is given by $\mathbf{T}^*(f_i) = \mathbf{V}(f_i)\mathbf{U}^H(f_i)$, where $\mathbf{U}(f_i), \mathbf{V}(f_i)$ are the left and right singular vectors of the matrix $\mathbf{A}^{(M)}(f_i, \hat{\boldsymbol{\theta}}) \left(\mathbf{A}^{(M)}(f_{\mathrm{ref}}, \hat{\boldsymbol{\theta}})\right)^H$. Once a set of focused measurements are obtained, they can be coherently combined to allow for the use of traditional narrow-band techniques like MUSIC or ESPRIT to get a refined estimate of the DOA's.

With recent advances in sparsity-based methods, further innovations to the Wideband DOA problem have been developed and studied [11, 13]. A new approach called DD-F-OG (Dynamic-Dictionary Focused Off-Grid) that combines focusing with sparsity-based DOA estimation was proposed in [12]. However, DD-F-OG still relies on the explicit construction of focusing matrices, whose quality is dependent on the initial DOA estimates.

III. INITIALIZATION-FREE IMPLICIT FOCUSING

In this section, we present a novel focusing method which overcomes the following restrictions present in the previously discussed methods: 1) our method is initialization-free, not requiring any potentially inaccurate DOA estimates 2) our method is implicitly formed, not requiring the construction of any focusing matrices. This is achieved by casting focusing as a rank minimization problem. We begin by providing theoretical guarantees for the extrapolation of low-frequency f_{low} to higher-frequency f_{low} for some integer f_{low} is a procedure we call *Initialization-Free Implicit Focusing* (IF²) for the general focusing of measurements if_{low} to if_{low} .

A. Theoretical Guarantees

Given an integer l, define

$$\mathbf{x}^{(l)}(f_i) := \mathbf{A}^{(l)}(f_i, \boldsymbol{\theta})\mathbf{s}(f_i) \tag{6}$$

Using this notation, the noiseless measurements from M sensors at frequency f_i can be written

$$\mathbf{x}^{(M)}(f_i) = \mathbf{A}^{(M)}(f_i, \boldsymbol{\theta})\mathbf{s}(f_i) \tag{7}$$

For an integer $1 \leq P < M$, measurements $\mathbf{x}^{(M)}(f_i)$ can be arranged to form a $P \times (M - P + 1)$ Hankel matrix

$$\mathcal{H}_{P}(\mathbf{x}^{(M)}(f_{i})) := \begin{bmatrix} x_{1} & x_{2} & \cdots & x_{M-P+1} \\ x_{2} & x_{3} & \cdots & x_{M-P+2} \\ \vdots & \vdots & \ddots & \vdots \\ x_{P} & x_{P+1} & \cdots & x_{M} \end{bmatrix}$$
(8)

where x_j is the jth entry of $\mathbf{x}^{(M)}(f_i)$. It can be shown that $\mathcal{H}_P(\mathbf{x}^{(M)}(f_i))$ will admit a Vandermonde decomposition [14]

$$\mathcal{H}_{P}(\mathbf{x}^{(M)}(f_{i})) = \mathbf{A}^{(P)}(f_{i}, \boldsymbol{\theta})\mathbf{S}\left(\mathbf{A}^{(M-P+1)}(f_{i}, \boldsymbol{\theta})\right)^{T}$$
(9)

where $S = \text{diag}(s(f_i))$, and $(\cdot)^T$ denotes the transpose. Let $[M] := \{1, \dots, M\}$ for some integer M.

Lemma 1. If $K \leq \min(P, M - P + 1)$, then $rank(\mathcal{H}_P(\mathbf{x}^{(M)}(f_i))) = K$, and any column of $\mathcal{H}_P(\mathbf{x}^{(M)}(f_i))$ can be uniquely represented as a linear combination of its first K columns.

Proof. From the decomposition in (9), both $\mathbf{A}^{(P)}(f_i, \boldsymbol{\theta})$ and $\mathbf{A}^{(M-P+1)}(f_i, \boldsymbol{\theta})$ are Vandermonde with distinct DOA's, and $K \leq \min(P, M-P+1)$

$$rank(\mathbf{A}^{(P)}(f_i, \boldsymbol{\theta})) = rank(\mathbf{A}^{(K)}(f_i, \boldsymbol{\theta})) = K$$
 (10)

The first K columns of $\mathcal{H}_P(\mathbf{x}^{(M)}(f_i))$ have the form $\mathcal{H}_P(\mathbf{x}^{(M)}(f_i))_{:,1:K} = \mathcal{H}_P(\mathbf{x}^{(M)}_{[P+K-1]}(f_i)) = \mathbf{A}^{(P)}(f_i, \boldsymbol{\theta}) \mathbf{S} \left(\mathbf{A}^{(K)}(f_i, \boldsymbol{\theta})\right)^T$ which can be verified to

be rank K due to the Vandermonde structure. Thus, the first K columns form a linearly independent set. Note that $\operatorname{rank}(\mathcal{H}_P(\mathbf{x}^{(M)}(f_i))) \leq K$, due to (9). Therefore, $\operatorname{rank}(\mathcal{H}_P(\mathbf{x}^{(M)}(f_i))) = K$ and the first K columns serve as a basis for $R(\mathcal{H}_P(\mathbf{x}^{(M)}(f_i)))$.

We now move on to prove the main theorem of this paper.

Theorem 1. Consider measurements $\mathbf{x}^{(M)}(f_i)$ of the form (7) with $K < \frac{M}{2}$. Then for any integer N > M, $P = \lceil \frac{N}{2} \rceil$, and $\Omega = [M]$, the solution to the rank minimization problem

$$\hat{\mathbf{y}}^{(N)} = \arg\min_{\mathbf{y}^{(N)} \in \mathbb{C}^N} rank(\mathcal{H}_P(\mathbf{y}^{(N)})), \text{ s.t. } \mathbf{y}_{\Omega}^{(N)} = \mathbf{x}^{(M)}(f_i)$$
(11)

satisfies $\hat{\mathbf{y}}^{(N)} = \mathbf{x}^{(N)}(f_i)$, where $\mathbf{x}^{(N)}(f_i)$ is given by (6) (with l = N) and it represents the extrapolated measurements.

Proof. From the constraint $\hat{\mathbf{y}}_{[M]}^N = \mathbf{x}^{(M)}(f_i)$, $\mathcal{H}_P(\hat{\mathbf{y}}^{(N)})$ contains a rank K top left sub-matrix

$$\mathcal{H}_{P}(\hat{\mathbf{y}}^{(N)}) = \begin{bmatrix} \mathcal{H}_{C}(\mathbf{x}^{(M)}) & \times \\ \times & \times \end{bmatrix}$$
(12)

where $C = \lceil \frac{M}{2} \rceil$, and from (9) $\mathcal{H}_C(\mathbf{x}^{(M)}) = \mathbf{A}^{(C)}(f_i, \boldsymbol{\theta}) \mathbf{S} \left(\mathbf{A}^{(M-C+1)}(f_i, \boldsymbol{\theta}) \right)^T$. Since there is a rank-K block $\mathcal{H}_C(\mathbf{x}^{(M)})$ contained in $\mathcal{H}_P(\hat{\mathbf{y}}^{(N)})$ we have rank $(\mathcal{H}_P(\hat{\mathbf{y}}^{(N)})) \geq K$. Recall that, from (9), $\mathcal{H}_P(\mathbf{x}^{(N)}(f_i))$ will admit Vandermonde decomposition

$$\mathcal{H}_{P}(\mathbf{x}^{(N)}(f_{i})) = \mathbf{A}^{(P)}(f_{i}, \boldsymbol{\theta})\mathbf{S}\left(\mathbf{A}^{(N-P+1)}(f_{i}, \boldsymbol{\theta})\right)^{T}$$
(13)

Since $K < \frac{M}{2}$ and N > M, (13) satisfies Lemma 1, $\operatorname{rank}(\mathcal{H}_P(\mathbf{x}^{(N)}(f_i))) = K$. Thus $\mathbf{x}^{(N)}(f_i)$ is a feasible point and attains the minimum rank K. Any optimal solution $\hat{\mathbf{y}}^{(N)}$ of (11) must satisfy $\operatorname{rank}(\mathcal{H}_P(\hat{\mathbf{y}}^{(N)})) = K$.

We will now provide a proof that $\hat{\mathbf{y}}^{(N)} = \mathbf{x}^{(N)}(f_i)$ through induction. Suppose the first M+j-1 entries of $\hat{\mathbf{y}}^{(N)}$ and $\mathbf{x}^N(f_i)$ are equal

$$\hat{\mathbf{y}}_{[M+j-1]}^{(N)} = \mathbf{x}_{[M+j-1]}^{(N)}(f_i)$$
(14)

i.e. for $D_j = \lceil \frac{M+j-1}{2} \rceil$ the following top left $D_j \times (M+j-D_j)$ sub-matrices of $\mathcal{H}_P(\hat{\mathbf{y}}^{(N)})$ and $\mathcal{H}_P(\mathbf{x}^{(N)}(f_i))$ satisfy

$$\mathcal{H}_{D_j}(\hat{\mathbf{y}}_{[M+j-1]}^{(N)}) = \mathcal{H}_{D_j}(\mathbf{x}_{[M+j-1]}^{(N)}(f_i))$$
(15)

The base case for induction (j = 1) is given by the constraint of (11).

Now for j > 1, consider the case where M+j-1 is odd. The $D_j \times (M+j-D_j+1)$ sub-matrix $\mathcal{H}_{D_j}(\hat{\mathbf{y}}_{[M+j]}^{(N)})$ of $\mathcal{H}_P(\hat{\mathbf{y}}^{(N)})$ is one which contains an extra column to the right of $\mathcal{H}_{D_j}(\hat{\mathbf{y}}_{[M+j-1]}^{(N)})$

$$\mathcal{H}_{D_j}(\hat{\mathbf{y}}_{[M+j]}^{(N)}) = \begin{bmatrix} \mathcal{H}_{D_j-1}(\hat{\mathbf{y}}_{[M+j-2]}^{(N)}) & \mathbf{v} \\ x_{D_j}, \dots, x_{M+j-1} & \hat{y}_{M+j} \end{bmatrix}$$
(16)

where $\mathbf{v} = [x_{M+j-D_j+1}, \cdots, x_{M+j-1}]^T$. Note that rank $(\mathcal{H}_{D_j}(\hat{\mathbf{y}}_{[M+j]}^{(N)})) \leq K$ since it is a sub-matrix of $\mathcal{H}_P(\hat{\mathbf{y}}^{(N)})$, whose rank is K. Further from Lemma 1, the above matrix contains a rank-K block $\mathcal{H}_{D_j}(\hat{\mathbf{y}}_{[M+j-1]}^{(N)})$ with first K columns being linearly independent. Therefore, we can

conclude that rank $\left(\mathcal{H}_{D_j}(\hat{\mathbf{y}}_{[M+j]}^{(N)})\right) = K$, and its last column can be represented as a linear combination of first K columns:

$$\mathcal{H}_{D_j}(\hat{\mathbf{y}}_{[D_j+K-1]}^{(N)})\mathbf{c} = \begin{bmatrix} \mathbf{v} \\ \hat{y}_{M+j} \end{bmatrix}$$
 (17)

Similarly, by representing the last column of $\mathcal{H}_{D_j}(\mathbf{x}_{[M+j]}^{(N)}(f_i))$ we have:

$$\mathcal{H}_{D_j}(\mathbf{x}_{[D_j+K-1]}^{(N)}(f_i))\mathbf{d} = \begin{bmatrix} \mathbf{v} \\ x_{M+j} \end{bmatrix}$$
 (18)

As a result of the induction assumption (14)

$$\mathcal{H}_{D_j-1}(\hat{\mathbf{y}}_{[M+j-1]}^{(N)}) = \mathcal{H}_{D_j-1}(\mathbf{x}_{[M+j-1]}^{(N)}(f_i))$$
(19)

Since $K < \frac{M}{2} < D_j$, we apply Lemma 1, the first K columns $\mathcal{H}_{D_j-1}(\mathbf{x}_{[D_j+K-2]}^{(N)}(f_i))$ of $\mathcal{H}_{D_j-1}(\hat{\mathbf{y}}_{[M+j-1]}^{(N)})$ are linearly independent. By removing the last row from (17),(18) we have:

$$\mathbf{v} = \mathcal{H}_{D_j - 1} \left(\hat{\mathbf{y}}_{[D_j + K - 2]}^{(N)} \right) \mathbf{c} = \mathcal{H}_{D_j - 1} \left(\mathbf{x}_{[D_j + K - 2]}^{(N)} (f_i) \right) \mathbf{d}$$
$$\mathcal{H}_{D_j - 1} \left(\mathbf{x}_{[D_j + K - 2]}^{(N)} (f_i) \right) (\mathbf{c} - \mathbf{d}) = 0 \Rightarrow \mathbf{c} = \mathbf{d}$$

Finally, since $\mathbf{c} = \mathbf{d}$, from (15),(17) we have $\hat{\mathbf{y}}_{[M+j]}^{(N)} = \mathbf{x}_{[M+j]}^{(N)}(f_i)$. Similar arguments as above (starting from (16)) can be repeated when M+j-1 is even by adding a row instead of a column in (16). Thus by induction over $1 \leq j \leq N-M$, we have $\hat{\mathbf{y}}^{(N)} = \mathbf{x}^{(N)}(f_i)$.

B. Proposed Approach

We propose an alternative focusing method that does not involve finding focusing matrices $\mathbf{T}(f_i)$, for the relevant frequency bins. Signals of the form (1) can be implicitly focused to different frequencies by exploiting the structure of the measurement matrix $\mathbf{A}(f_i, \boldsymbol{\theta})$ in a procedure motivated by the result of Theorem 1.

Given the measurement $\mathbf{x}^{(M)}(f)$ at frequency $f \in [f_{\text{low}}, f_{\text{high}}]$ as defined in (1), then corresponding measurements focused to a frequency f' will then have the form

$$\mathbf{x}_{\text{focus}}^{(M)}(f, f') = \mathbf{A}^{(M)}(f', \boldsymbol{\theta})\mathbf{s}(f)$$
 (20)

Let $\alpha_k = e^{j\pi(f_{\text{low}}/f_{\text{high}})\sin(\theta_k)}$. Then it can be readily verified that elements of the manifold at f_{low} are given by $\left[\mathbf{A}^{(M)}(f_{\text{low}}, \boldsymbol{\theta})\right]_{m,k} = \alpha_k^m$. Any other frequency f_i for integer $i \geqslant 1$ will have the form $f_i = if_{\text{low}}$. We can write manifolds as sub-sampling of $\mathbf{A}^{(iM)}(f_{\text{low}}, \boldsymbol{\theta})$

$$\left[\mathbf{A}^{(M)}(f_i, \boldsymbol{\theta})\right]_{m,k} = \left[\mathbf{A}^{(iM)}(f_{\text{low}}, \boldsymbol{\theta})\right]_{im,k} \tag{21}$$

for $1 \leq m \leq M$, $1 \leq k \leq K$

1) Focusing from f_{low} to if_{low} : Informed by (21), the focused measurements will have elements which are subsampled from extrapolated measurements $\mathbf{x}^{(iM)}(f_{low})$

$$\left[\mathbf{x}_{\text{focus}}^{(M)}(f_{\text{low}}, if_{\text{low}})\right]_{m} = \left[\mathbf{x}^{(iM)}(f_{\text{low}})\right]_{im}$$
(22)

for $1 \leq m \leq M$. We propose to determine $\mathbf{x}^{(iM)}(f_{\text{low}}) \in \mathbb{C}^{iM}$ by solving the following rank minimization problem

$$\hat{\mathbf{y}}^{(iM)} = \arg\min_{\mathbf{y}^{(iM)}} \quad \operatorname{rank}(\mathcal{H}_{P_i}(\mathbf{y}^{(iM)}))$$
s.t.
$$\|\mathbf{y}_{[M]}^{iM} - \mathbf{x}^M(f_{\text{low}})\|_2 \leq \epsilon$$

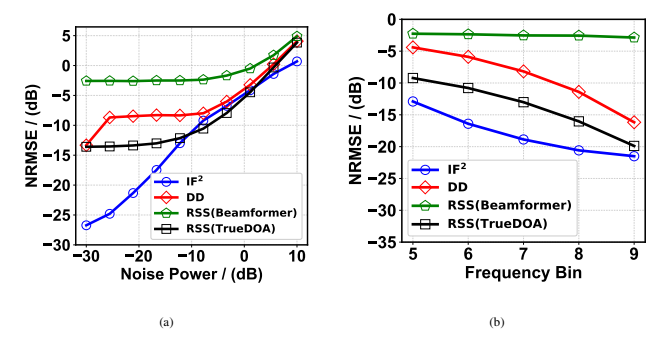


Fig. 1: (a) Average NRMSE VS Noise Power for measurements from all frequency bins focused to bin 10 using various methods. (b) NRMSE vs. Frequency for bins 5 to 9 when focused to bin 10 using different methods in presence of noise with $\sigma^2=2.15\times 10^{-2}$.

where $P_i = \lceil iM/2 \rceil$. As shown Theorem 1, solving (23) with noiseless measurements ($\epsilon = 0$) will indeed recover $\mathbf{x}^{(iM)}(f_{\text{low}})$, i.e. $\hat{\mathbf{y}}^{(iM)} = \mathbf{x}^{(iM)}(f_{\text{low}})$. We obtain an estimate for focused measurements $\hat{\mathbf{x}}^{(M)}_{\text{focus}}(f_{\text{low}}, if_{\text{low}})$ by sub-sampling $\hat{\mathbf{y}}^{(iM)}$ according to (22).

$$\left[\hat{\mathbf{x}}_{\text{focus}}^{(M)}(f_{\text{low}}, f_i)\right]_m = \left[\hat{\mathbf{y}}^{(iM)}\right]_{im}$$
(24)

2) Focusing from if_{low} to jf_{low} : In this case, we start with measurements $\mathbf{x}^{(M)}(if_{low})$. We propose to focus from if_{low} to $jf_{low}(j>i)$ in two steps.

First, perform an interpolation procedure to obtain intermediate measurements $\mathbf{x}^{(iM)}(f_{\text{low}})$ by solving the following rank minimization problem

$$\hat{\mathbf{y}}^{(iM)} = \underset{\mathbf{y}^{(iM)}}{\min} \quad \operatorname{rank}(\mathcal{H}_{P_i}(\mathbf{y}^{(iM)}))$$
s.t.
$$\|\mathbf{y}_{\Omega_i}^{(iM)} - \mathbf{x}^{(M)}(f_{\text{low}})\|_2 \leqslant \epsilon$$

where $\Omega_i = \{pi \mid 0 . Second, the extrapolation procedure from Section III-B1 may now be performed to focus <math>\hat{\mathbf{y}}^{(iM)} = \hat{\mathbf{x}}^{(iM)}(f_{\text{low}})$ to jf_{low} and yield an estimate $\hat{\mathbf{x}}_{\text{focus}}^{(M)}(f_i, f_j)$. If (25) succeeds, then this step will also succeed through Theorem 1. In practice, solving (23) and (25) is difficult, and known to be NP-Hard. For this reason, we will use nuclear norm $(\|\cdot\|_*)$, which is a convex surrogate for rank.

IV. SIMULATIONS

In our first set of simulations, we consider K=2 and M=12 sensors. We only consider the scenario with p=1 in our simulations. We assume the DOA's lie on a $N_g=100$ uniformly spaced grid between 0° and 60° . On this grid, the 2 DOA's correspond to grid indices 30 and 60. We consider D=32 DFT bins, with the wideband signals occupying frequency bins 5 to 10. In simulations, complex Gaussian noise is added to the measurements. Signal amplitudes for each DOA and DFT bin are drawn from a uniform distribution between 1 and 2. Our method is compared to DD-F (DD-F-OG) which is presented in [12] after 4 iterations of re-focusing. For initial DOA estimates in DD-F, a coarser grid of 50 points between 0° and 60° was used, with initial step-size $r=3^\circ$. Only the first step of DD-F is performed to predict DOA's for refocusing, since

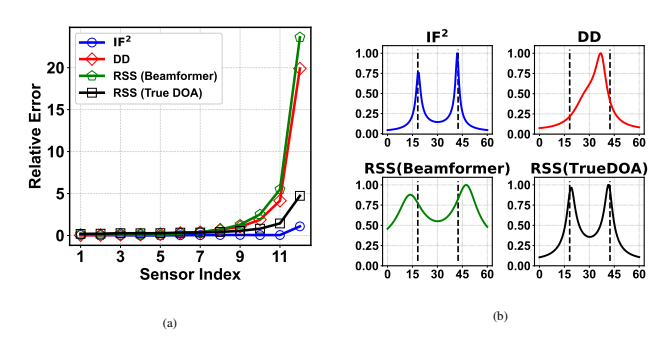


Fig. 2: (a) Relative error per entry of example measurement from bin 5 focused to bin 10, $\sigma^2 = 0.01$. (b) Example of DOA recovery. MUSIC is applied to focused measurements from various focusing methods with additive noise of $\sigma^2 = 0.01$. True DOA's indicated with dashed black line.

the grid bias vector $\alpha_K = 0$ for our on-grid setting. We also compare against the classic RSS using a simple beamformer for initial DOA estimates. RSS focusing using the true DOA's is also provided as a baseline for comparison. Our error metric is the Normalized Root Mean Squared Error (NRMSE) given by NRMSE($\hat{\mathbf{x}}_{\text{focus}}, \mathbf{x}_{\text{focus}}) = \frac{\|\hat{\mathbf{x}}_{\text{focus}}(f, f') - \mathbf{x}_{\text{focus}}(f, f')\|_2}{\|\mathbf{x}_{\text{focus}}(f, f')\|_2}$ where $\mathbf{x}_{\text{focus}}(f, f')$ and $\hat{\mathbf{x}}_{\text{focus}}(f, f')$ denote the true and predicted focused measurements respectively. Fig. 1a shows the resulting average RNMSE errors for focusing bins 5-9 to bin 10 vs. noise power, averaged over 100 Monte Carlo runs. Unlike other methods, IF2 focusing is initialization-free, and doesn't show bias to initial DOA estimates. Hence its error does not saturate as SNR increases. IF² also demonstrates resiliency in lower SNR regimes, both outperforming DD-F and beamforming techniques, and obtaining performance closer to RSS with knowledge of true DOA's. Fig. 1b shows the NRMSE errors that result in focusing measurements with noise power $\sigma^2 = 2.15 \times 10^{-2}$ to frequency bin 10. For all the bins, IF² focusing consistently yields the best performance, even outperforming RSS with knowledge of the true DOA's.

Another experiment was performed with K=3 DOA grid indices 60, 80, 95 and $\sigma^2=0.01$. Fig. 2a shows the relative error for each measurement entry when focusing a bin 5 signal to bin 10 with $\sigma^2=0.01$ noise. IF² clearly demonstrates the ability to focus with lower error even in the presence of noise. Finally, an experiment to evaluate DOA recovery was performed with K=2 DOA grid indices 30, 70. Fig. 2b shows recovered DOA's using the same DOA estimation method, namely narrowband MUSIC, on the focused measurements provided from various algorithms. RSS with Beamformer DOA estimates does not exhibit good performance. DD-F also does not demonstrate reliable results. Both RSS with knowledge of True DOA's, and IF² are able to sufficiently resolve the DOA's.

V. CONCLUSION

We proposed a novel method for implicitly focusing array manifolds at different frequencies to a reference frequency, which can be used for wideband DOA estimation. Unlike existing methods, our technique requires no initial DOA estimates and theoretical guarantees for exact focusing are also established. Numerical simulations demonstrate the superiority of our methods compared to past and recent focusing techniques.

²In Section IV, we provide simulations which demonstrate that the interpolation step succeeds.

REFERENCES

- [1] N. Garcia, H. Wymeersch, E. G. Larsson, A. M. Haimovich, and M. Coulon, "Direct localization for massive mimo," *IEEE Transactions on Signal Processing*, vol. 65, no. 10, pp. 2475–2487, 2017.
- [2] L. C. Godara, "Application of antenna arrays to mobile communications. ii. beam-forming and direction-of-arrival considerations," *Proceedings of the IEEE*, vol. 85, no. 8, pp. 1195–1245, 1997.
- [3] H. Krim and M. Viberg, "Two decades of array signal processing research: The parametric approach," *IEEE signal processing magazine*, vol. 13, no. 4, pp. 67–94, 1996.
- [4] R. Schmidt, "Multiple emitter location and signal parameter estimation," *IEEE transactions on antennas and propagation*, vol. 34, no. 3, pp. 276–280, 1986.
- [5] R. Roy and T. Kailath, "Esprit-estimation of signal parameters via rotational invariance techniques," *IEEE Transactions on acoustics, speech, and signal process*ing, vol. 37, no. 7, pp. 984–995, 1989.
- [6] S. Nannuru, A. Koochakzadeh, K. L. Gemba, P. Pal, and P. Gerstoft, "Sparse bayesian learning for beamforming using sparse linear arrays," *The Journal of the Acousti*cal Society of America, vol. 144, no. 5, pp. 2719–2729, 2018.
- [7] M. Wax, T.-J. Shan, and T. Kailath, "Spatio-temporal spectral analysis by eigenstructure methods," *IEEE transactions on acoustics, speech, and signal processing*, vol. 32, no. 4, pp. 817–827, 1984.
- [8] Y.-S. Yoon, L. M. Kaplan, and J. H. McClellan, "Tops: New doa estimator for wideband signals," *IEEE Transactions on Signal processing*, vol. 54, no. 6, pp. 1977–1989, 2006.
- [9] H. Wang and M. Kaveh, "Coherent signal-subspace processing for the detection and estimation of angles of arrival of multiple wide-band sources," *IEEE Trans*actions on Acoustics, Speech, and Signal Processing, vol. 33, no. 4, pp. 823–831, 1985.
- [10] H. Hung and M. Kaveh, "Focussing matrices for coherent signal-subspace processing," *IEEE Transactions on Acoustics, Speech, and Signal Processing*, vol. 36, no. 8, pp. 1272–1281, 1988.
- [11] Q. Shen, W. Cui, W. Liu, S. Wu, Y. D. Zhang, and M. G. Amin, "Underdetermined wideband doa estimation of off-grid sources employing the difference co-array concept," *Signal Processing*, vol. 130, pp. 299–304, 2017.
- [12] W. Cui, Q. Shen, W. Liu, and S. Wu, "Low complexity doa estimation for wideband off-grid sources based on re-focused compressive sensing with dynamic dictionary," *IEEE Journal of Selected Topics in Signal Processing*, vol. 13, no. 5, pp. 918–930, 2019.
- [13] Q. Shen, W. Liu, W. Cui, S. Wu, Y. D. Zhang, and M. G. Amin, "Focused compressive sensing for underdetermined wideband doa estimation exploiting high-order difference coarrays," *IEEE Signal Processing Letters*, vol. 24, no. 1, pp. 86–90, 2016.

[14] W. Liao and A. Fannjiang, "Music for single-snapshot spectral estimation: Stability and super-resolution," *Applied and Computational Harmonic Analysis*, vol. 40, no. 1, pp. 33–67, 2016.